

There remains the possibility that Fe_2P_2 ring inversion in $[(\mu\text{-DMP})\text{Fe}(\text{CO})_3]_2$ is influenced by enhanced Fe-P $d\pi\text{-}d\pi$ bonding. If such π bonding is important and if it does influence the inversion process, it does so without any apparent structural consequences (apart from the short Fe-P and long Fe-C bonds). The question of whether this is possible cannot be resolved by a purely structural investigation. However, Burdett³ has argued that the equilibrium geometry in $[\text{R}_2\text{PFe}(\text{CO})_3]_2$ complexes results largely from a balance between Fe-P and Fe-Fe interactions. It seems very unlikely that any electronic effect sufficient to influence the inversion rate (by altering the relative energies of the molecular orbitals so as to reduce the barrier to inversion) would fail to affect these interactions and thus the molecular geometry as well.

Thus it appears, as has been suggested earlier,¹ that neither steric nor electronic effects seem to provide a satisfactory explanation for the relative ease of inversion of the Fe_2P_2 ring in $[(\mu\text{-DMP})\text{Fe}(\text{CO})_3]_2$. This strengthens our confidence in the hypothesis that the rate of this process is enhanced by coupling with the more rapid inversion of the phosphorinane ring.¹ However, it is not possible to evaluate this possibility

using static structural data; this will require further NMR studies of other compounds.

Acknowledgment. This work was supported by the assistance of the Emory University Computing Center. The authors thank Dr. J. A. Bertrand of Georgia Institute of Technology for generously providing access to his facilities.

Registry No. $[(\mu\text{-DMP})\text{Fe}(\text{CO})_3]_2$, 65150-25-6.

Supplementary Material Available: Listing of structure factor amplitudes (18 pages). Ordering information is given on any current masthead page.

References and Notes

- (1) C. M. Bartish and C. S. Kraihanzel, *Inorg. Chem.*, **17**, 735 (1978).
- (2) W. Clegg, *Inorg. Chem.*, **15**, 1609 (1976).
- (3) J. K. Burdett, *J. Chem. Soc., Dalton Trans.*, 423 (1977).
- (4) R. J. Doedens and J. A. Ibers, *Inorg. Chem.*, **6**, 204 (1967).
- (5) "International Tables for X-ray Crystallography", Vol. IV, Kynoch Press, Birmingham, England, 1974: (a) pp 72-98; (b) pp 149-150.
- (6) P. M. Treichel, W. K. Dean, and J. L. Calabrese, *Inorg. Chem.*, **12**, 2908 (1973).
- (7) R. E. Dessy, A. L. Rheingold, and G. D. Howard, *J. Am. Chem. Soc.*, **94**, 746 (1972).
- (8) J. Grobe, *Z. Anorg. Allg. Chem.*, **361**, 32 (1968).

Contribution from the Department of Chemistry,
University of South Carolina, Columbia, South Carolina 29208

Crystal and Molecular Structure of a Colored Intermediate from the Reaction of Tetramethylthiourea and Copper(2+) (Dichlorobis(tetramethylthiourea)copper(II))

E. A. H. GRIFFITH, W. A. SPOFFORD, III, and E. L. AMMA*

Received July 28, 1977

The crystal and molecular structure of dichlorobis(tetramethylthiourea)copper(II) has been determined. The structure consists of isolated molecules separated by ordinary van der Waals distances. The environment of the metal atom is that of a distorted tetrahedron with Cu-Cl distances of 2.241 (6) and 2.234 (6) Å and Cu-S distances of 2.314 (7) and 2.316 (6) Å. The Cl-Cu-Cl angle is 145.0 (3)° and the S-Cu-S angle is 140.1 (3)° while the Cl-Cu-S angles are 98° or less. The orientation of the tetramethylthiourea groups is determined by chlorine-methyl repulsions. The tetramethylthiourea group is distorted from planarity due to methyl-methyl interference. A consistent reaction scheme and structure relationship is proposed including this intermediate and related intermediates as well as the structurally diverse reaction products of thiourea and cupric ion in aqueous solution. The crystals are monoclinic: $P2_1$; $a = 9.464$ (2), $b = 8.550$ (1), $c = 11.532$ (2) Å; $\beta = 105.56$ (4)°; $\rho_o = 1.46$, $\rho_c = 1.47$ g cm⁻³; $Z = 2$. The structure was solved by standard heavy-atom methods and refined by full-matrix least squares including anisotropic temperature factors to an R of 0.064 with 1133 reflections.

Introduction

In the reaction of thiourea $[\text{SC}(\text{NH}_2)_2]$, tu, with metal ions, such as Fe^{3+} or Cu^{2+} , which are capable of setting up a redox system in aqueous solution, transient intermediates of unusual color are frequently observed.¹ In particular, Cu^{2+} with thiourea and substituted thioureas gives a rose to purple transient intermediate in which the exact color is dependent upon the thiourea derivative and is especially anion dependent. These colored intermediates may further react to a series of polynuclear Cu(I) intermediates such as $\text{Cu}_4\text{S}_6^{4+}$, $\text{Cu}_6\text{S}_9^{4+2}$ ($\text{S} =$ a particular thiourea ligand) which ends in an infinite polymer $(\text{Cu}_4\text{S}_9^{4+})_x$.³ Alternatively these colored intermediates may proceed directly to the following: polymeric end products such as $(\text{Cu}_4\text{S}_{10}^{4+})_x$,⁴ which contain Cu-S bridged six-membered Cu_3S_3 rings; linear Cu-S bridged polymers $(\text{CuS}_2\text{Cl})_x$,⁵ Cu-S bridged dimers such as $\text{Cu}_4\text{S}_6^{2+}$,^{6,7} isolated planar three-coordinate Cu(I) entities, CuS_3^+ ,⁸ or isolated tetrahedral Cu(I) moieties, CuS_3Cl^0 (for details vide infra). The exact end product is dependent upon steric factors and concentration of the sulfur ligand as well as the anion. With the ligand tetramethylthiourea, the chloride anion, and Cu^{2+} we have been able to isolate the colored intermediate and preserve a

few crystals for a sufficient period of time to carry out a single-crystal structure analysis. We wish to report the details¹⁰ of that analysis here and relate the structure of this intermediate to the known structures of many of the reaction products of this process.

Experimental Section

Preparation. Tetramethylthiourea (1.3 g (0.01 mol) in 60 mL of H_2O) was mixed with approximately 1 L of crushed ice. A deep burgundy color developed as soon as $\text{CuCl}_2 \cdot 2\text{H}_2\text{O}$ [0.4 g (0.0023 mol) in 400 mL of H_2O] was added slowly with rapid stirring. The color gradually faded to colorless (~ 2 h) and the solution was maintained thereafter at room temperature. After 2 days a small amount of free sulfur was filtered off and the solution was allowed to evaporate almost to dryness. A reddish brown oil developed in which ruby red crystals formed in large clumps or aggregates. Diffraction-grade fragments were immediately cleaved from these clumps since the crystalline material is unstable if allowed to remain in the oil or left in contact with open air. Accordingly, a number of samples were coated with petroleum jelly and sealed in Lindemann capillaries for diffraction studies.

X-Ray Data. Preliminary Weissenberg and precession photographic data showed that the crystals were monoclinic with systematic absences of $k = 2n + 1$ for $0k0$, which is compatible for either space group

Table I. Final Atomic Positional and Thermal Parameters with Errors^a

Atom	x	y	z	β_{11}	β_{22}	β_{33}	β_{12}	β_{13}	β_{23}
Cu	0.2158 (3)	0.7500 (x) ^b	0.2692 (2)	123 (4)	117 (4)	64 (2)	4 (4)	40 (2)	-8 (3)
Cl(1)	0.3771 (7)	0.7976 (8)	0.1624 (5)	179 (10)	171 (12)	94 (6)	-35 (8)	80 (6)	-19 (6)
Cl(2)	0.0007 (7)	0.8196 (8)	0.2990 (5)	115 (8)	206 (11)	83 (6)	35 (8)	24 (5)	-7 (6)
S(1)	0.1317 (9)	0.5022 (8)	0.2048 (6)	242 (14)	139 (11)	105 (7)	-62 (10)	99 (8)	-43 (7)
S(2)	0.3660 (7)	0.8747 (8)	0.4353 (5)	117 (9)	153 (10)	82 (6)	-31 (8)	46 (6)	-34 (6)
C(1)	0.214 (3)	0.444 (2)	0.094 (2)	131 (34)	101 (33)	61 (2)	-6 (27)	33 (21)	0 (20)
N(1)	0.299 (2)	0.314 (2)	0.113 (2)	213 (40)	144 (33)	87 (2)	49 (30)	27 (22)	23 (20)
N(2)	0.184 (2)	0.516 (2)	-0.011 (1)	155 (31)	123 (29)	49 (15)	-4 (25)	25 (17)	6 (18)
C(3)	0.304 (3)	0.208 (3)	0.009 (3)	260 (56)	151 (50)	152 (34)	-2 (37)	141 (38)	-51 (29)
C(4)	0.366 (3)	0.246 (5)	0.238 (2)	187 (42)	323 (60)	77 (22)	57 (60)	44 (24)	15 (44)
C(5)	0.302 (3)	0.528 (3)	-0.077 (2)	169 (41)	183 (45)	51 (19)	2 (35)	60 (23)	-31 (24)
C(6)	0.058 (3)	0.624 (3)	-0.052 (2)	162 (46)	163 (42)	98 (29)	45 (36)	2 (27)	18 (27)
C(2)	0.283 (2)	0.872 (3)	0.551 (2)	96 (29)	62 (28)	73 (20)	-13 (25)	24 (20)	-30 (21)
N(3)	0.218 (2)	0.736 (3)	0.578 (1)	192 (32)	111 (29)	64 (15)	24 (31)	38 (18)	39 (21)
N(4)	0.279 (2)	0.997 (2)	0.615 (2)	154 (31)	107 (28)	60 (16)	-16 (24)	41 (18)	-19 (18)
C(7)	0.081 (3)	0.741 (4)	0.618 (2)	173 (39)	223 (46)	105 (23)	-9 (46)	100 (25)	39 (37)
C(8)	0.262 (4)	0.585 (3)	0.546 (3)	341 (75)	56 (35)	85 (28)	0 (39)	56 (37)	-2 (24)
C(9)	0.305 (4)	1.159 (3)	0.569 (3)	214 (58)	118 (44)	191 (45)	-40 (39)	65 (39)	-9 (34)
C(10)	0.280 (4)	0.996 (3)	0.744 (2)	315 (64)	202 (48)	78 (25)	-48 (52)	89 (32)	-32 (30)

^a Anisotropic temperature factors are of the form $\exp[-(\beta_{11}h^2 + \beta_{22}k^2 + \beta_{33}l^2 + 2\beta_{12}hk + 2\beta_{13}hl + 2\beta_{23}kl) \times 10^4]$. ^b (x) fixed by space group.

$P2_1$,¹¹ as determined structurally (vide infra), or space group $P2_1/m$. The many-faceted crystal fragments were mounted such that the unique axis was parallel to the ϕ axis on a card-controlled Picker diffractometer and aligned by variations of well-known techniques.¹² A least-squares fit of the χ , ϕ , and 2θ angles of 29 accurately centered reflections was used to calculate an operational matrix and to determine the lattice parameters at room temperature with Mo $K\alpha$ radiation, λ 0.71068 Å. Crystal data: $P2_1$, $a = 9.464$ (2) Å, $b = 8.550$ (1) Å, $c = 11.532$ (2) Å, $\beta = 105.56$ (4)°.¹³ The calculated density of 1.47 g cm⁻³ for $Z = 2$ molecules/cell is in good agreement with the experimental density of 1.46 (2) g cm⁻³ measured by flotation in carbon tetrachloride-chlorobenzene solution. The linear absorption coefficient using Mo $K\alpha$ radiation is $\mu = 14.4$ cm⁻¹, and no absorption corrections were made.¹⁴

Data Collection. Because of extensive decomposition in the X-ray beam, the data were collected utilizing two crystals of dimensions 0.042 × 0.014 × 0.019 cm and 0.066 × 0.029 × 0.019 cm, respectively. A total of 1950 independent reflections were measured (888 reflections for crystal 1, 1247 for crystal 2; includes standards and duplicates) in the hkl and $\bar{h}kl$ octants by a standard θ - 2θ scan at a rate of 1°/min. Crystal 1 was scanned 1.4° in 2θ (84 s scan) and crystal 2, 1.5° (90 s scan). Unfiltered Mo $K\alpha$ (λ 0.71068 Å) was used¹⁵ except for zonal and low-angle reflections where a Zr filter was used. Backgrounds were estimated by a stationary count of 40 s at either end of the scan. Reflections were considered absent if the integrated intensity was less than $2[t_i(B_1 + B_2)]^{1/2}$ where t_i for crystal 1 was 1.05 and t_i for crystal 2 was 1.125. By this criterion 1133 reflections were retained as being nonzero. A standard reflection (-4,3,2) was measured every tenth reflection to ensure operational stability, to monitor the crystal decomposition, and to provide a basis for scaling the data as decomposition proceeded. Intensity loss for the standard reflection had a linear correlation with exposure time and data collection on crystal 1 was discontinued when the intensity had dropped to roughly 30%¹⁶ of the initial intensity. A section of the data from crystal 1 was remeasured on crystal 2 for comparison and scaling and integrated intensities of these sections agreed within an average of 5–8%. This is the same order of agreement observed within 15 symmetry-related reflections, hkl , $\bar{h}kl$. The takeoff angle, source-to-crystal, and crystal-to-counter distances were 3.7°, 18 cm, and 23 cm, respectively. The peak width at half-peak height for an average intensity reflection was 0.4° in 2θ indicating a mosaic spread such that all the reflection was counted during the scan. The counting rate never exceeded 5000 counts/s, and no attenuators were used. The usual Lorentz polarization corrections were made and the intensities reduced to structure factors.

Structure Solution and Refinement

The structure was solved by standard heavy-atom methods¹⁷ and the correct space group was shown to be $P2_1$.¹⁸ The structure was refined by full-matrix least squares¹⁹ including anisotropic temperature factors. The function minimized in the least-squares refinement was $\sum(|F_o| - |F_c|)^2$ (unit weights) and the scattering factors used were from Cromer and Waber.²⁰ The effects of the anomalous dispersion

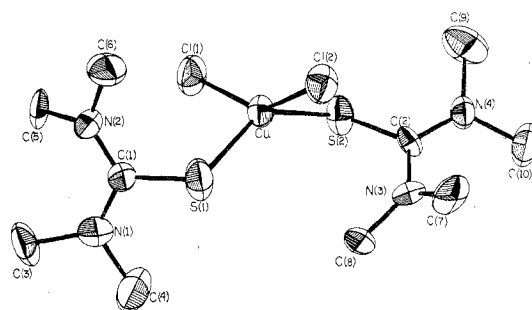


Figure 1. An ORTEP plot¹⁶ of the dichlorobis(tetramethylthiourea)copper(II) molecule. The notation is consistent with angle and distance data in Table II. Ellipsoids are drawn at the 50% probability level. The twist of the NC_2 terminal groups is clearly seen. H atoms are not included.

from the Cu, S, and Cl atoms were included in the structure factor calculations by addition to F_c ; the values for $\Delta f'$ and $\Delta f''$ were those given by Cromer.^{22a} The anisotropic refinement based on 1133 reflections and 114 variables gradually converged to a final value of $R_1 = 0.064$ and $R_2 = 0.072$.^{22b} The final parameter shifts were 0.1 σ or less, and a final difference Fourier gave no indication of the positions of the methyl hydrogens and was generally featureless.

The final tabulation of observed and calculated structure factors is filed elsewhere together with the calculated structure factors for the unobserved data which were not used in the structure refinement.²³ Final atomic coordinates and thermal parameters are listed in Table I. Interatomic distances, angles, dihedral angles between normals to planes, and their errors were computed from the parameters and variance-covariance²⁴ matrix of the last cycle of least squares and are found in Table II. Table III presents least-squares planes, and root-mean-square components of thermal displacement are listed in Table IV.²⁴

Structure Description

The structure of dichlorobis(tetramethylthiourea)copper(II) consists of isolated molecules separated by ordinary van der Waals distances. The environment about the Cu(II) species is that of a distorted tetrahedron.^{25,26} The tetrahedral distortion is that of a flattening perpendicular to the approximate twofold axis passing through the Cu atom and the midpoint of the intramolecular Cl-Cl and S-S vectors. This distortion gives rise to the opening of the Cl-Cu-Cl angle to 145.0 (3)° and the S-Cu-S angle to 140.1 (3)° whereas the Cl-Cu-S angles are decreased from the tetrahedral value to less than 98° (Table II). The Cu-Cl and Cu-S distances are normal values. The Cu-S-C angle of $\sim 109^\circ$ indicates that the

Table II. Interatomic Distances (Å) and Angles (deg) with Esd

Bonded Distances			
Cu-Cl(1)	2.241 (6)	Cu-S(1)	2.314 (7)
Cu-Cl(2)	2.234 (6)	Cu-S(2)	2.316 (6)
S(1)-C(1)	1.74 (2)	S(2)-C(2)	1.72 (2)
C(1)-N(1)	1.35 (3)	C(2)-N(3)	1.39 (3)
N(1)-C(3)	1.51 (3)	N(3)-C(8)	1.44 (3)
N(1)-C(4)	1.53 (3)	N(3)-C(7)	1.48 (3)
C(1)-N(2)	1.31 (3)	C(2)-N(4)	1.30 (3)
N(2)-C(5)	1.51 (3)	N(4)-C(9)	1.53 (3)
N(2)-C(6)	1.48 (3)	N(4)-C(10)	1.49 (3)
Nonbonded Distances <4.0 Å			
Cl(2)-N(2)	3.72 (2)	C(6)-C(1)	3.70 (3)
Cl(2)-C(5)	3.74 (2)	C(6)-N(1)	3.65 (3)
Cl(2)-C(6)	3.78 (3)	C(6)-C(3)	3.67 (3)
C(6)-S(1)	3.89 (3)		
Angles			
Cl(1)-Cu-Cl(2)	145.0 (3)	Cl(2)-Cu-S(1)	92.5 (3)
Cl(1)-Cu-S(1)	102.5 (2)	Cl(2)-Cu-S(2)	97.6 (2)
Cl(1)-Cu-S(2)	90.8 (2)	S(1)-Cu-S(2)	140.1 (3)
Cu-S(1)-C(1)	108.5 (8)	Cu-S(2)-C(2)	109.2 (8)
S(1)-C(1)-N(1)	119 (2)	S(2)-C(2)-N(3)	121 (1)
S(1)-C(1)-N(2)	121 (2)	S(2)-C(2)-N(4)	121 (2)
N(1)-C(1)-N(2)	120 (2)	N(3)-C(2)-N(4)	119 (2)
C(1)-N(1)-C(3)	121 (2)	C(2)-N(3)-C(7)	121 (2)
C(1)-N(1)-C(4)	123 (3)	C(2)-N(3)-C(8)	121 (2)
C(3)-N(1)-C(4)	115 (2)	C(7)-N(3)-C(8)	116 (2)
C(1)-N(2)-C(5)	119 (2)	C(2)-N(4)-C(9)	121 (2)
C(1)-N(2)-C(6)	123 (2)	C(2)-N(4)-C(10)	125 (2)
C(5)-N(2)-C(6)	116 (2)	C(9)-N(4)-C(10)	113 (2)
Dihedral Angles between Planes			
Cl(1)-Cu-S(2)	53.0 (2)	Cu-S(1)-C(1)	37.4 (5)
Cl(2)-Cu-S(1)		Cu-S(2)-C(2)	
Cl(1)-Cu-S(1)	49.5 (2)	N(3)-C(2)-N(4)	27 (3)
Cl(2)-Cu-S(2)		C(9)-N(4)-C(10)	
Cl(1)-Cu-Cl(2)	85.6 (2)	N(3)-C(2)-N(4)	149 (3)
S(1)-Cu-S(2)		C(8)-N(3)-C(9)	
Cl(1)-Cu-Cl(2)	67.3 (5)	S(1)-C(1)-N(1)	146 (2)
Cu-S(1)-C(1)		C(1)-N(1)-C(3)	
Cl(1)-Cu-Cl(2)	75.5 (5)	S(1)-C(1)-N(1)	19 (3)
Cu-S(2)-C(2)		C(1)-N(1)-C(4)	
S(2)-C(2)-N(4)	18 (3)	S(1)-C(1)-N(2)	5 (3)
C(2)-N(4)-C(9)		C(1)-N(1)-N(2)	
S(2)-C(2)-N(4)	149 (2)	S(1)-C(1)-N(2)	148 (2)
C(2)-N(4)-C(10)		C(1)-N(2)-C(5)	
S(2)-C(2)-N(3)	144 (2)	S(1)-C(1)-N(2)	14 (3)
C(2)-N(3)-C(7)		C(1)-N(2)-C(6)	
S(2)-C(2)-N(3)	24 (3)	C(1)-N(1)-N(2)	32 (3)
C(2)-N(3)-C(8)		N(2)-C(5)-C(6)	
Cu-S(2)-C(2)	45 (1)	Cu-S(1)-C(1)	63.5 (9)
S(2)-C(2)-N(3)-N(4)		S(1)-C(1)-N(1)-N(2)	

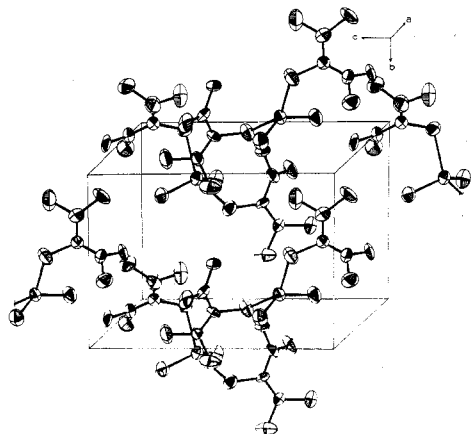


Figure 2. An ORTEP³⁶ packing diagram of the complex of Figure 1. The hydrogen atoms have not been shown for reasons of simplicity. The ellipsoids are plotted at the 50% probability level. The origin is in the front upper right-hand corner.

Table III. Equation of Least-Squares Plane of the Type $Ax + By + Cz - D = 0$

Plane no.	Atoms defining plane	Deviations from plane, (Å)	
1	S(1)	0.008	$A = -0.7128$
	C(1)	-0.029	$B = -0.5920$
	N(1)	0.010	$C = -0.3761$
	N(2)	0.011	$D = 3.8428$
2	S(2)	0.001	$A = -0.7214$
	C(2)	-0.004	$B = 0.2692$
	N(3)	0.001	$C = -0.6381$
	N(4)	0.002	$D = 2.601$
3	C(1)	-0.030	$A = 0.8714$
	N(1)	0.080	$B = 0.4901$
	C(3)	-0.025	$C = -0.0190$
	C(4)	-0.025	$D = -3.3787$
4	C(1)	-0.034	$A = -0.3286$
	N(2)	0.091	$B = -0.7778$
	C(5)	-0.028	$C = -0.5359$
	C(6)	-0.029	$D = 4.042$
5	C(2)	0.023	$A = -0.3533$
	N(3)	-0.064	$B = 0.0509$
	C(7)	0.020	$C = -0.9341$
	C(8)	0.021	$D = 5.7096$
6	C(2)	-0.025	$A = -0.9445$
	N(4)	0.065	$B = 0.0877$
	C(9)	-0.019	$C = -0.3166$
	C(10)	-0.020	$D = 2.1797$

Table IV. Root-Mean-Square Displacements along Principal Axes of Thermal Ellipsoids (Å)

	1	2	3
Cu	0.176 (4)	0.213 (4)	0.233 (4)
Cl(1)	0.185 (7)	0.237 (8)	0.306 (8)
Cl(2)	0.205 (8)	0.227 (8)	0.289 (8)
S(1)	0.189 (9)	0.210 (9)	0.349 (9)
S(2)	0.188 (8)	0.200 (8)	0.275 (8)
C(1)	0.189 (30)	0.195 (31)	0.231 (29)
N(1)	0.199 (28)	0.246 (26)	0.313 (27)
N(2)	0.173 (28)	0.214 (25)	0.257 (25)
C(3)	0.158 (36)	0.262 (34)	0.371 (34)
C(4)	0.211 (30)	0.266 (37)	0.356 (39)
C(5)	0.123 (38)	0.265 (32)	0.272 (30)
C(6)	0.199 (38)	0.263 (33)	0.301 (36)
C(2)	0.129 (40)	0.201 (31)	0.227 (29)
N(3)	0.149 (33)	0.234 (28)	0.287 (24)
N(4)	0.167 (29)	0.206 (26)	0.260 (26)
C(7)	0.136 (39)	0.290 (37)	0.315 (37)
C(8)	0.145 (44)	0.227 (35)	0.374 (39)
C(9)	0.197 (40)	0.305 (41)	0.342 (40)
C(10)	0.183 (40)	0.267 (34)	0.371 (35)

thiourea sulfur is bound to Cu(II) primarily via a lone pair of electrons in a nonbonding sp^2 sulfur orbital. However, there is some contribution from the π electrons of the S-C bond as well since the dihedral angles between the Cu-S-C and S-C-N₂ planes are 45 and 64°. The use of the sp^2 orbitals and electron pair is the most common mode of binding of thiourea to Cu(I)⁹ as well as to other transition metals.^{27,28} However, a number of cases also exist where S-C π electrons are almost exclusively used in transition metals²⁹ as well as in Cu(I) complexes.^{5,6,30} The S-C distances are comparable to those found for free thiourea at 1.746 (9) Å from the neutron data³¹ and 1.720 (9) Å from the X-ray data.³² Within our relatively large error the central C-N distances of the thiourea groups are normal with a mean of 1.34 (4) Å. The terminal C-N distances are normal at 1.48–1.53 Å except for N(3)-C(8) which is short at 1.44 (3) Å. We see no reason for this shortening and attribute it to limitations in the intensity data.

The orientation of the thiourea groups relative to the central $CuCl_2S_2$ unit appears to be determined primarily by nonbonded interactions between methyl groups and chlorine atoms as well

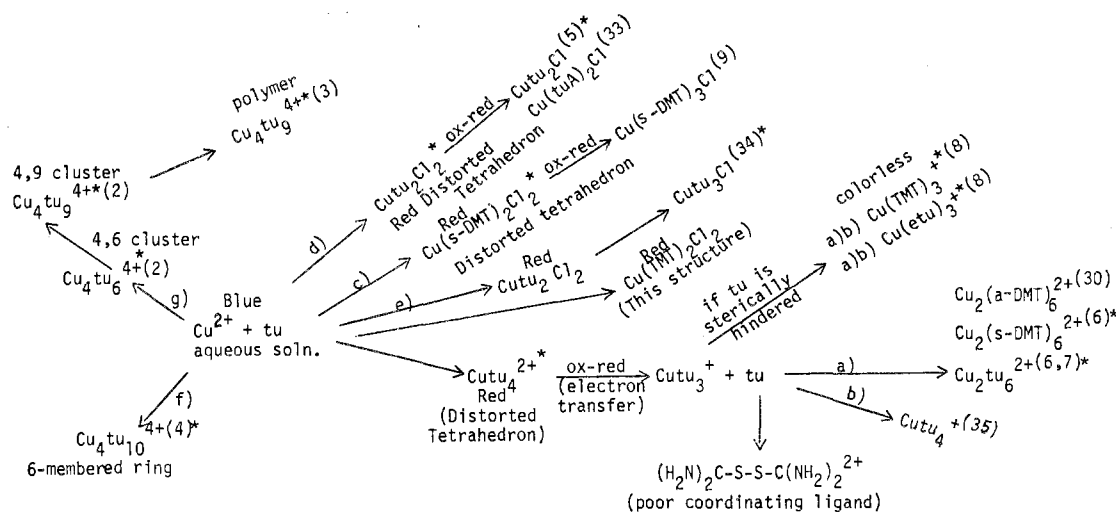


Figure 3. Summary of Cu^{2+} and thiourea reactions: (*) Structure known from X-ray crystallography or inferred from known structures; (a) 1:4 molar ratio Cu^{2+}/tu starting stoichiometry, noncoordinating anion BF_4^- , SiF_6^{2-} , ClO_4^- ; (b) 1:4 molar ratio starting stoichiometry, noncoordinating anion gives (a) + (b); (c) 1:4 molar ratio Cu^{2+}/tu , coordinating ligand such as Cl^- ; (d) 1:3 molar ratio Cu^{2+}/tu , coordinating ligand such as Cl^- ; (e) 1:4 Cu^{2+}/tu with Cl^- , nonsterically hindered tu; (f) 1:3 Cu^{2+}/tu with BF_4^- or SiF_6^{2-} (no red intermediate); (g) excess Cu^{2+}/tu with NO_3^- (no red intermediate). Key: tu = thiourea, TMT = tetramethylthiourea, s-DMT = *N,N'*-dimethylthiourea, a-DMT = *N,N,N',N'*-dimethylthiourea, tuA = 2-thiouracil, etu = ethylenethiourea. Notes: $\text{Cu}_2(\text{tu})_6^{2+}$, sulfur-bridged dimer with four-coordinate Cu^+ ; $\text{Cu}(\text{tu})_4^+$, tetrahedral four-coordinate Cu^+ monomer; $\text{Cu}(\text{TMT})_3^+$, three-coordinate planar Cu^+ ; $\text{Cu}(\text{etu})_3^+$, three-coordinate planar Cu^+ ; $\text{Cu}(\text{tu})_3\text{Cl}$, infinite chain of tetrahedral sulfur-bonded Cu^+ ; $\text{Cu}(\text{s-DMT})_3\text{Cl}$, isolated tetrahedral Cu^+ ; $\text{Cu}(\text{tu})_2\text{Cl}$, three-coordinate planar Cu^+ ; $\text{Cu}(\text{tuA})_2\text{Cl}$, three-coordinate planar Cu^+ ; $\text{Cu}_4(\text{tu})_{10}(\text{SiF}_6)_2$, polymer containing six-membered rings and bridged by Cu-S bonds; $\text{Cu}_4(\text{tu})_6(\text{NO}_3)_4$, tetrahedral cluster of three-coordinate planar Cu^+ contained within an octahedron of bonded S atoms; $\text{Cu}_4(\text{tu})_9(\text{NO}_3)_4$, cluster of four Cu^+ containing three four-coordinate metals and one three-coordinate metal derived from $\text{Cu}_4(\text{tu})_6$ by adding three thiourea groups; $\text{Cu}_4(\text{tu})_9(\text{NO}_3)_4$, infinite polymer containing a variety of types of sulfur-bridged, Cu^+ species.

as methyl-methyl contacts (Table II). The tetramethylthiourea groups are placed approximately between the chlorine ligands to minimize the Cl-CH₃ repulsion but the methyl-methyl group repulsion across the central CuS_2Cl_2 unit twists these groups $\sim 37^\circ$ relative to one another (see dihedral angles, Table II). Nonbonded methyl-methyl interactions also cause the nonhydrogen framework of the tetramethylthiourea groups to be nonplanar (see least-squares plane Table III) whereas the SCN_2 central framework remains planar. However, within experimental error for each of the C-N(CH₃)₂ fragments the central carbon, a nitrogen, and its associated terminal carbon atoms are planar. Hence, the distortion of the tetramethylthiourea groups from planarity can be viewed as rotations of planes about C(central)-N bonds of 11-32° to minimize steric repulsions.

Discussion

In the light of the present structural results and the color similarity of all the transient-colored intermediates in the reaction of thiourea and substituted thioureas with cupric ion in cold aqueous solution, it seems reasonable to postulate that they are all tetrahedral or more likely distorted tetrahedral species. They may be $\text{Cu}(\text{tu})_4^{2+}$, $\text{Cu}(\text{tu})_3\text{X}^+$, or $\text{Cu}(\text{tu})_2\text{X}_2$ where tu is thiourea or a substituted thiourea and X is an anion. The general reaction scheme for the reaction of Cu^{2+} and thiourea may now be summarized with the known stereochemistries as shown in Figure 3. It is seen that the reaction products passing through the red intermediates can be rationalized in terms of the distorted tetrahedral structure for the red intermediate. The rationale for the $\text{Cu}(\text{tu})_3^+$ intermediate is the isolation and structure determination of the three-coordinate planar Cu^+ in $\text{Cu}(\text{TMT})_3^+$ and $\text{Cu}(\text{etu})_3^+$,⁸ as well as a logical intermediate for the dimers $\text{Cu}_2(\text{tu})_6^{2+}$.^{6,7,30} An additional interesting feature is that the three-coordinate planar Cu^+ arises under a variety of circumstances such as in the two clusters $\text{Cu}_4(\text{tu})_6^{4+}$,² $\text{Cu}_4(\text{tu})_9^{4+2}$ as well as the isolated molecules mentioned above. It appears that there is little difference energetically between four-coordinate tetrahedral Cu^+ and three-coordinate planar Cu^+ , at

least in the presence of soft electron donors, and therefore it may be said that the environment of Cu(I) in the presence of soft donors is very flexible. This may be an important property for copper in copper enzymes.

Acknowledgment. This research was supported in part by National Institutes of Health Grant GM13985

Registry No. $\text{Cu}(\text{TMT})_2\text{Cl}_2$, 29863-37-4.

Supplementary Material Available: A listing of structure factor amplitudes (6 pages). Ordering information is given on any current masthead page.

References and Notes

- D. A. Zatko and B. Kratochvil, *Anal. Chem.*, **40**, 2120 (1968).
- E. A. H. Griffith, G. W. Hunt, and E. L. Amma, *J. Chem. Soc., Chem. Commun.*, 432 (1976).
- R. G. Vranka and E. L. Amma, *J. Am. Chem. Soc.*, **88**, 4270 (1966).
- A. G. Gash, E. H. Griffith, W. A. Spofford, III, and E. L. Amma, *J. Chem. Soc., Chem. Commun.*, 256 (1973).
- W. A. Spofford, III, and E. L. Amma, *Acta Crystallogr., Sect. B*, **26**, 1474 (1970).
- I. F. Taylor, Jr., M. S. Weininger, and E. L. Amma, *Inorg. Chem.*, **13**, 2835 (1974).
- F. Hanic and E. Durcanska, *Inorg. Chim. Acta*, **3**, 293 (1969).
- M. S. Weininger, G. W. Hunt, and E. L. Amma, *J. Chem. Soc., Chem. Commun.*, 1140 (1972).
- R. L. Girling and E. L. Amma, *Inorg. Chem.*, **10**, 335 (1971).
- W. A. Spofford, III, E. A. H. Griffith, and E. L. Amma, *Chem. Commun.*, 533 (1970).
- N. F. M. Henry and K. Lonsdale, Ed., "International Tables for X-Ray Crystallography", Vol. I, Kynoch Press, Birmingham, England, 1952, pp 78, 92.
- W. R. Busing and H. A. Levy, *Acta Crystallogr.*, **22**, 457 (1967). This system has since been redesigned and rebuilt. The diffractometer is operated by a PDP-8 networked to a PDP-11/40 to an IBM 370/168 and U B matrices are calculated either on the PDP-11/40 or on the IBM 370/168.
- The least-squares fit to compute the lattice dimensions is a program based upon ref 12 by W. A. Spofford, III, for the IBM 1620. This calculation is now performed on the PDP-11/40.
- The errors due to crystal decomposition and the subsequent scaling using only one standard reflection probably outweigh the errors due to lack of absorption corrections. In addition, ill-formed chips coated with Vaseline are not suited for analytical absorption corrections.
- This is a somewhat unconventional technique but has been successful in 15 or more structure solutions. It improves intensity statistics but it may well have contributed to the rapid demise of the crystals in the X-ray beam.

- (16) This may seem like an extremely high decomposition level for intensity data collection, but we never had more than three crystals of diffraction quality. One was used up for the photographic data and the two remaining were used for intensity data collection.
- (17) Patterson and electron density syntheses were calculated using "ERFR-3, a Three-Dimensional Fourier Summation Program Adapted for the IBM 7040 from ERFR-2 of Sly, Shoemaker, and van den Hende", by D. R. Harris. These (by different programs) calculations are now done on the IBM 370/168.
- (18) In space group $P2_1$ (a polar space group) in the presence of anomalous dispersion it is possible to determine the chirality of the crystal. No attempt was made to do so in the present instance for the following reasons: (1) the anomalous dispersion correction for Cu with Mo $K\alpha$ radiation is small; (2) two different crystals were used for the intensity data and they were not sufficiently well formed so that it could be certain they were both mounted in an identical manner. However, four possibilities could have been tested involving the two sign permutations on k for each crystal. This was rejected out of hand as a waste of computing time because of the general limitations of the intensity data as well as the fact that the different crystals represented data from different 2θ shells. Under these conditions it would have been better to have neglected $\Delta f''$ in the refinement, the general shortcoming of the intensity data indicated in text.
- (19) W. R. Busing, K. O. Martin, and H. A. Levy, "ORFLS, a Fortran Crystallographic Least-Squares Program", Report ORNL-TM-305, Oak Ridge National Laboratory, Oak Ridge, Tenn., 1962. The version incorporates modifications by W. A. Spofford, III.
- (20) D. T. Cromer and J. T. Waber, *Acta Crystallogr.*, **18**, 104 (1965).
- (21) J. A. Ibers and W. C. Hamilton, *Acta Crystallogr.*, **17**, 781 (1964).
- (22) (a) D. T. Cromer, *Acta Crystallogr.*, **18**, 17 (1965); (b) $R_1 = \sum(|F_o| - |F_c|)/\sum|F_o|$; $R_2 = \sum(F_o - F_c)^2/\sum(F_o)^2$.
- (23) Supplementary material.
- (24) W. R. Busing, K. O. Martin, and H. A. Levy, "ORFFE, a Fortran Crystallographic Function and Error Program", Report ORNL-TM-306, Oak Ridge National Laboratory, Oak Ridge, Tenn., 1964. The version incorporates modifications by W. A. Spofford, III.
- (25) F. A. Cotton and G. Wilkinson, "Advanced Inorganic Chemistry", 3rd ed, Wiley, New York, N.Y., 1972, p 912, and references therein.
- (26) J. Gazo, *Pure Appl. Chem.*, **38**, 279 (1974).
- (27) J. E. O'Connor and E. L. Amma, *Inorg. Chem.*, **8**, 2367 (1969).
- (28) (a) R. L. Girling, K. K. Chatterjee, and E. L. Amma, *Inorg. Chim. Acta*, **7**, 557 (1973); (b) D. A. Berta, W. A. Spofford, III, P. Boldrini, and E. L. Amma, *Inorg. Chem.*, **9**, 136 (1970).
- (29) (a) W. A. Spofford, III, P. Boldrini, E. L. Amma, P. Carfagno, and P. G. Gentile, *Chem. Commun.*, **40** (1970); (b) W. A. Spofford, III, and E. L. Amma, *J. Cryst. Mol. Struct.*, **6**, 235 (1976).
- (30) M. S. Weinger, I. F. Taylor, Jr., and E. L. Amma, *Inorg. Nucl. Chem. Lett.*, **9**, 737 (1973).
- (31) M. M. Elcombe and J. C. Taylor, *Acta Crystallogr., Sect. A*, **24**, 410 (1968).
- (32) (a) M. R. Truter, *Acta Crystallogr.*, **22**, 536 (1967); (b) Z. V. Zvonkova, L. I. Astakhova, and V. P. Glushkova, *Kristallografiya*, **5**, 547 (1960).
- (33) (a) G. W. Hunt and E. L. Amma, *J. Chem. Soc., Chem. Commun.*, 869 (1973); (b) G. W. Hunt, E. A. H. Griffith and E. L. Amma, *Inorg. Chem.*, **15**, 2993 (1976).
- (34) (a) Y. Okaya, C. B. Knobler, and R. Pepinsky, *Z. Kristallogr., Kristallgeom., Kristallphys., Kristallchem.*, **111**, 385 (1959); (b) Y. Okaya and C. B. Knobler, *Acta Crystallogr.*, **17**, 928 (1964).
- (35) G. W. Hunt, N. W. Terry, III, and E. L. Amma, *Cryst. Struct. Commun.*, **3**, 523 (1974).
- (36) C. K. Johnson, "ORTEP, a Fortran Thermal-Ellipsoid Plot Program for Crystal Structure Illustrations", ORNL-3794, Oak Ridge National Laboratory, Oak Ridge, Tenn., 1965.

Contribution from the Department of Chemistry,
The University of Michigan, Ann Arbor, Michigan 48109

Platinum and Palladium Complexes of Thienylpyridine. 2. Quasi-Octahedral Divalent-Metal Compounds

T. J. GIORDANO, W. M. BUTLER, and P. G. RASMUSSEN*

Received September 27, 1977

In this paper we report the syntheses and structures of complexes of divalent platinum and palladium with 2-(2'-thienyl)pyridine (TP). The general formulas are $M(TP)_2X_2$ ($X^- = Br^-, Cl^-$). The crystal structure of $Pd(TP)_2Br_2$ was determined from three-dimensional X-ray diffraction data collected by counter methods. The compound $Pd(C_{18}H_{14}N_2S_2)Br_2$ was found to crystallize in the monoclinic space group $P2_1/c$ with $a = 6.328$ (1) Å, $b = 16.536$ (4) Å, $c = 9.267$ (2) Å, $\beta = 99.85$ (2)°, and $Z = 2$ molecules/cell. The structure was refined by standard methods to final $R_1 = 4.4\%$ and $R_2 = 4.8\%$ for 1244 nonzero reflections. The palladium atom is located on an inversion center and is coordinated to two nitrogen atoms (2.021 Å) and two bromine atoms (2.431 Å) in typical square-planar fashion. In addition, the two thiophene sulfur atoms are located above and below the coordination atom (3.05 Å), making the complex quasi-octahedral. The implications of this unusual geometry are discussed in the light of the structural and spectroscopic properties. The synthesis and characterization of *cis*- and *trans*- $Pd(TP)_2Cl_2$ and *trans*- $Pt(TP)_2Cl_2$ are also described. The geometries of these monomeric complexes have been determined by far-infrared measurements and analogy to the structure of $Pd(TP)_2Br_2$. The electronic spectra of the palladium complexes are similar to those of other four-coordinate, square-planar complexes of palladium(II). The electronic spectrum of the platinum complex contains an intense low-energy d-d band indicative of metal-thiophene axial interactions and is similar to the previously described complexes $Pt(TP)(TP-H)I$ and $Pt(TP)(TP-H)Br$. A thiophene-based band at 850 cm^{-1} in the infrared spectrum of the free ligand is not significantly shifted in the palladium complexes but is shifted to 875 cm^{-1} in the platinum complex. The data pertinent to the metal binding ability of thiophene are summarized, and estimates are made of the strength of this interaction.

Introduction

We have previously reported the results of our initial investigations on the ligating properties of 2-(2'-thienyl)pyridine (TP).¹ In that earlier paper we described the ease with which the thiophene moiety forms metal-carbon bonds by loss of a hydrogen (TP-H). We now report on a series of compounds of formula $M(TP)_2X_2$ ($M = Pd, Pt; X = Cl, Br$) in which no new carbon bonds are formed. In these compounds two thiophene groups are located above and below the coordination plane at somewhat ambiguous distances with respect to bonding.

The complexes of formula $M(TP)_2X_2$ are analogous to the well-known dihalobis(pyridine) complexes of platinum(II) and palladium(II). We have previously noted similarities of the electronic and infrared spectra of $Pt(TP)(TP-H)I$ and

$Pt(TP)(TP-H)Br$ with the spectrum of *trans*- $Pt(TP)_2Cl_2$, which we ascribed to interactions between the metal atom and a thiophene ring in an axial position. Here we will describe more fully the syntheses and characterizations of *trans*- $Pt(TP)_2Cl_2$, *cis*- and *trans*- $Pd(TP)_2Cl_2$, and *trans*- $Pd(TP)_2Br_2$, as well as the X-ray crystal structure of the latter.

These data provide some answers to questions regarding the binding tendency of thiophene, which were the original impetus for this work.

Experimental Section

Infrared spectra ($4000\text{--}450\text{ cm}^{-1}$), electronic spectra, conductivity measurements, and X-ray powder photographs were obtained by methods previously described.¹ Far-infrared spectra ($450\text{--}100\text{ cm}^{-1}$) were obtained on a Digilab Fourier transform spectrometer. A Nujol mull between polyethylene sheets was used for the sample and reference cells.